Skull Stripping of MRI Head Scans based on Chan-Vese Active Contour Model

K. Somasundaram[1] and P. Kalavathi[2]

Image Processing Lab, Department of Computer Science and Applications
Gandhigram Rural Institute, Gandhigram – 624 302, Tamilnadu, India

[1]somasundaramk@yahoo.com [2]pkalavathi.gri@gmail.com

Abstract— **Whole brain segmentation referred as skull stripping, it is an important process in neuriomage analysis. Automatic segmentation of brain tissues from magnetic resonance images (MRI) remains a challenging task due to variation in shape and size, use of different pulse sequences, overlapping signal intensities and imaging artifacts. Level sets and active contour methods have tremendous potential in the area of image segmentation. In this paper, we propose a new skull stripping algorithm for magnetic resonance images (MRI) of human head scans based on Chan-Vese active contour method. This is a fully automatic method for segmenting the brain from other non-brain tissues in T1, T2 and PD weighted MR images. The proposed method consists of two major processes. First we extracted the brain in the middle slice and then the brains in the remaining slices are extracted. In this method the binary form of the brain image is processed first to find the rough brain. The initial contour is drawn inside the rough brain portion to propagate the active contour. In our method the process of extracting the brain in the remaining slices were simplified by using the geometric similarities of the adjacent slice. The proposed method extracts the brain accurately in T1, T2 and PD weighted images. The result of the proposed method is compared with the standard manual skull stripping gold standard images and produced significant result. The experimental results indicate that the proposed method accurately extracted the brain which is comparable to that of BET and BSE using the IBSR and WBA datasets.**

Keywords— **Skull stripping, brain extraction method, active contour, magnetic resonance image(MRI), brain segmentation**

I. INTRODUCTION

Magnetic resonance imaging (MRI) is a most widely used imaging technique in the medical field. It is a noninvasive method and does not require ionizing radiation such as X-rays. It reveals information about the human soft tissue anatomy [1]. The MRI of head scans reveal the details of human brain and its surrounding tissues.

Skull stripping is the process of eliminating all non-brain tissues from brain images. It removes extra cerebral tissues such as skull, sclera, fat, skin etc, from the brain images. It is an essential pre-processing step in neuroimage analysis. However, the presence of image artifacts, anatomical variability, varying contrast properties and poor registration make this process a difficult one. The brain portion must be skull stripped before other image processing algorithms such as registration, tissue classification or compression can be applied [2]. A number of automated and semi-automated skull stripping algorithms are available in literature [3]. Each of the existing skull stripping technique has its own strengths and weaknesses [4].

Brain Extraction Tool (BET) [5] employs deformable model that evolves to fit the brain's surface by the application of a set of locally adaptive model forces. The Brain Surface Extraction (BSE) proposed by Shattuck et al.,[6] uses a combination of operations such as anisotropic diffusion filtering, Marr-Hildreth edge detection and morphological operations, to separate brain from non-brain tissues.

The Watershed Algorithm (WAT) [7] is an intensity based approach that operates under the assumption of white matter connectivity and segment the image into brain and non-brain components. But it often produces over segmentation and is sensitive to noise present in the image. A hybrid method for skull stripping, Hybrid Watershed Algorithm (HWA) proposed by Segonne et al., [8] works by combining the watershed techniques and a deformable surface model. This method first localizes a single white matter voxel in T1-weigthed image, and uses it to create a global minimum in the white matter before applying a watershed algorithm. Zhuang et al., [9] developed an automatic skull stripping algorithm called Model-based Level Set (MLS) based on active curve to remove the skull and intracranial tissues surrounding the brain in MR brain images. Skull stripping using Graph cuts (GCUT) [10] relies on graph theoretic image segmentation techniques to position cuts that serve to isolate and remove dura. A statistical shape model for automatic skull stripping of brain images proposed in [11] is based on surface model of the brain boundary and it is hierarchically represented by a set of overlapping surface patches, each of which has elastic property and deformation range that is learned from a training set.

Park and Lee [12] developed a skull stripping method for coronal T1-weighted images based on region growing. It aims to automatically detect two seed regions of the brain and non-brain by using a mask produced by morphological operations. Then the seed regions were expanded using 2D region growing algorithm. In [13] and [14] a fully automatic brain extraction algorithm using diffusion, run length encoding and region labeling were developed for skull stripping in T2 weighted axial MR brain images. Brummer [15] suggested that the geometric continuity of brain in a volume could be exploited in neighboring slices to select the regions corresponding to brain. Several studies have been reported for skull stripping based on anisotropic diffusion filter and morphological processing [16][17], seed growth and thresholding techniques [18], fuzzy-ASM based [19], and deformable surface and tissue classification [20]. Most of these methods are applicable to T1 weighted MR brain images, and does not extract the brain completely in all the slices. Moreover, none of these existing methods give

satisfactory performance when evaluated for large-scale data set. It is due to the complexity of the human brain, varying image contrast properties, image artifacts such as under-sampling, noise factor, variations in the image orientations and types. There appears to be no single method that works for all the three types of T1, T2 and PD weighted images.

In this paper we propose a fully automatic method for skull stripping in T1, T2 and PD weighted MRI of head scans for all the three orientations axial, coronal and sagittal based on Chan-Vese (CV) active contour model. Experimental results using our method on T1, T2 and PD weighted images, obtained from IBSR and WBA datasets, show that our method gives better results than that of the two popular existing skull stripping methods. The remaining part of the paper is organized as follows: In Section II, we present the methods and the materials used in our experiments. The experimental results and discussion are given Section III. In Section IV, the conclusion is given.

II. METHODS AND MATERIALS

2.1 Methods

The proposed skull stripping algorithm is a fully automatic two stage method. In Stage -1, we extract the brain portion from the middle slice of the brain volume. In MRI of head scan, there exists a similarity in the shapes of the brain portion between two successive slices [13]. We make use of these similarities to extract the brain portion in the remaining slices in Stage-2.

2.1.1 Stage-1: Brain Extraction from Middle Slices (BEMS)

In MRI of head scans, the brain portion in the middle slice appears as a single largest connected component (LCC). This characteristic makes it possible to extract the brain region easily in the middle slices of the stack. After finding the brain mask for the middle slice, it can be used as a reference to extract brain region from other slices.

The BEMS comprise of several operations: binarization, brain area selection, smoothing, initial contour detection and segmentation by CV model. The flowchart of the Stage-1 is shown in Figure1.

The middle slice lying at the position M = N/2, where N is the total number of slices of the brain volume is first taken for processing. Using Ostu's method [21] an intensity threshold value (T) is obtained. Using this intensity threshold T, a binary image is obtained as:

$$g(x,y) = \begin{cases} 1 & if \quad f(x,y) \geq T \\ 0 & otherwise \end{cases} \tag{1}$$

where, *f(x,y)* is the intensity of the input image.

The binary image g contains several isolated regions. It is known that in the middle slices, the brain region is the LCC. We therefore, search for LCC in g. For this, the connected regions are labeled as 1,2 etc., using run length encoding technique [22]. Hence g may contain several sub-regions and therefore it can be expressed as:

$$g = \sum_{i=1}^{n} R(i) \tag{2}$$

where R(i) is the i[th] isolated region. We then calculate the area of i[th] region $R(i)$ as $R_A(i)$.

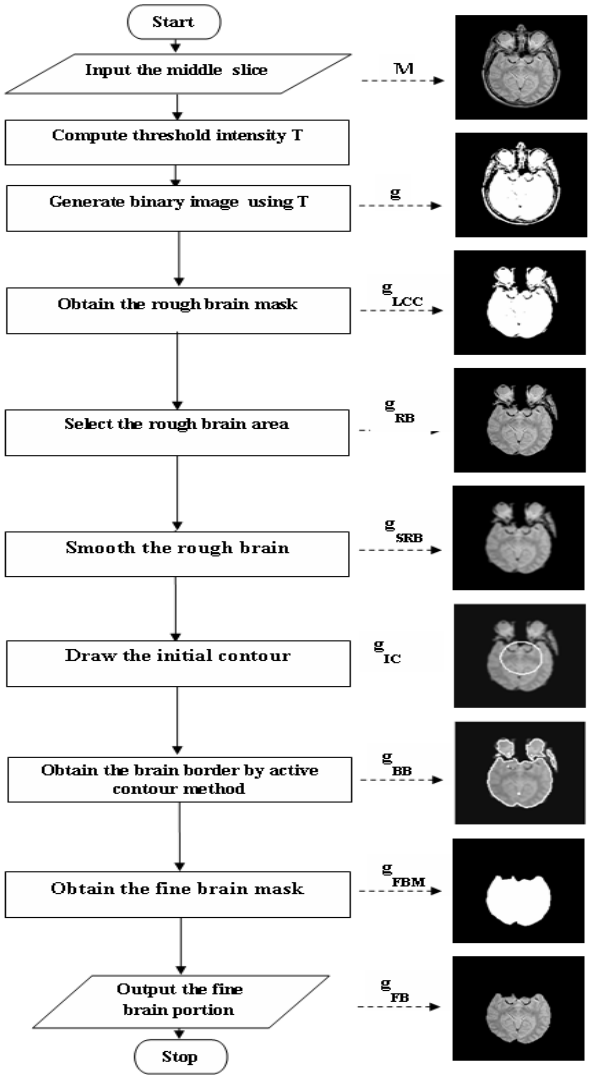

Figure 1: Flowchart of Stage-1

The LCC in g_E is obtained by:

$$g_{LCC} = R(\arg\max_{1 \leq i \leq n}(R_A(i))) \tag{3}$$

Using the selected g_{LCC} the rough brain area is selected as:

$$g_{RB} = \begin{cases} f(x,y) & if \ g_{LCC}(x,y) = 1 \\ 0 & otherwise \end{cases} \tag{4}$$

The edges of the rough brain g_{RB} are then smoothed to get g_{SRB}. Most border detection techniques are sensitive to small discontinuities at the boundaries of the object. Therefore we perform smoothing process prior to applying brain border detection by CV contouring technique to reduce the level of noise, and to enhance the local discontinuities at the brain boundaries. By smoothing the brain border is enhanced and at the same time the number of internal contours in the brain image is reduced. Smoothing is done using a circular averaging filter of radius *r* with in a square matrix of side 2**r* +1. A circular averaging filter with radius *r*=2.5 is shown Figure 2.

$$h_{circ}[x, y] = \frac{1}{21}\begin{bmatrix} 01110 \\ 11111 \\ 11111 \\ 11111 \\ 01110 \end{bmatrix}$$

Figure 2: Circular averaging filter with r=2.5

We then draw the initial contour (IC) on the fine brain area. The radius of the IC is computed by taking the average of the distance from the centre of g_{SRB} towards the brain border in the four directions, (x, y, -x, -y). The radius *r* is calculated as:

$$r = \frac{D}{2}, \quad where, \quad D = \frac{\sum d_i}{4}, \quad i = 1 \ldots 4. \tag{5}$$

where, d_i represents the distance from the center of the extracted brain to the border on right$_{(i=1)}$, top$_{(i=2)}$, left$_{(i=3)}$,and bottom$_{(i=4)}$. The IC is drawn with the mid point of the brain portion extracted as its centre point at (x_c, y_c) with a radius of *r* and is denoted as g_{IC}.

We used Chan-Vese active contour (CV) without edges [23] to find the brain border image g_{BB} on the smoothed rough brain image g_{SRB} by using g_{IC} as initial contour. This model efficiently identifies the contour that has smooth boundaries. It can do this because the evaluation of the curve does not depend on gradient information, so the week edge does not affect the final segmentation. The formulation of the CV focused on bimodal images. In the bimodal model, it is assumed that an image consists of two regions, C_f (foreground) and C_b (background) of approximately piecewise-constant distinct intensity values. If the region to be segmented is represented by C_f, then a curve C can be evolved to reach the boundary of C_f by minimizing the following energy.

$$E(C) = \mu Length(C) + v Area(inside(C)) + F_1(C) + F_2(C) \tag{6}$$

$F_1(C)$ and $F_2(C)$ are defined as follows:

$$F_1(C) = \lambda_1 \int_{inside(C)} \left| g_{SRB}(x, y) - c_1 \right|^2 dydx \tag{7}$$

$$F_2(C) = \lambda_2 \int_{outside(C)} \left| g_{SRB}(x, y) - c_2 \right|^2 dydx \tag{8}$$

where, $\mu \geq 0$, $v \geq 0, \lambda_1, \lambda_2 > 0$ are fixed parameters. In our method we assigned $\mu = 0.2$, $v = 0, \lambda_1, = \lambda_2 = 1$. C represents the curve, and the variables c_1 and c_2 represent the average intensities inside and outside the curve respectively. If the curve C is inside the region to be segmented, represented by intensity C_f, then $F_1(C) \approx 0$ and $F_2(C) > 0$. If the curve C is outside C_f , then $F_1(C) > 0$ and $F_2(C) \approx 0$. Only when the curve is on the boundary of the region will have $F_1(C) \approx 0$ and $F_2(C) \approx 0$.

The holes in the g_{BB} is filled using hole filling algorithm [22] to produce g_{HBB} . The fine brain mask g_{FBM} is generated by finding the intersecting connected component (CC) regions between g_{FBB} and IC. During connected component (CC) analysis, those CCs that overlaps with IC will be taken as brain portion and others will be discarded, i.e., only the CCs that satisfy the condition:

$$CC(x, y) \cap IC(x, y) \neq \phi \tag{9}$$

will be taken as brain portion. From g_{FBM} the fine brain area g_{FB} is selected as:

$$g_{FB} = \begin{cases} f(x, y) & if \ g_{FBM}(x, y) = 1 \\ 0 & otherwise \end{cases} \tag{10}$$

2.1.2. Stage-2: Brain Extraction in the Remaining Slices

After extracting the brain portion in the middle slice, we move upward and downward in the slice stack to extract the brain regions in the lower and upper slices. The overall flowchart of the proposed method is shown in Figure 3.

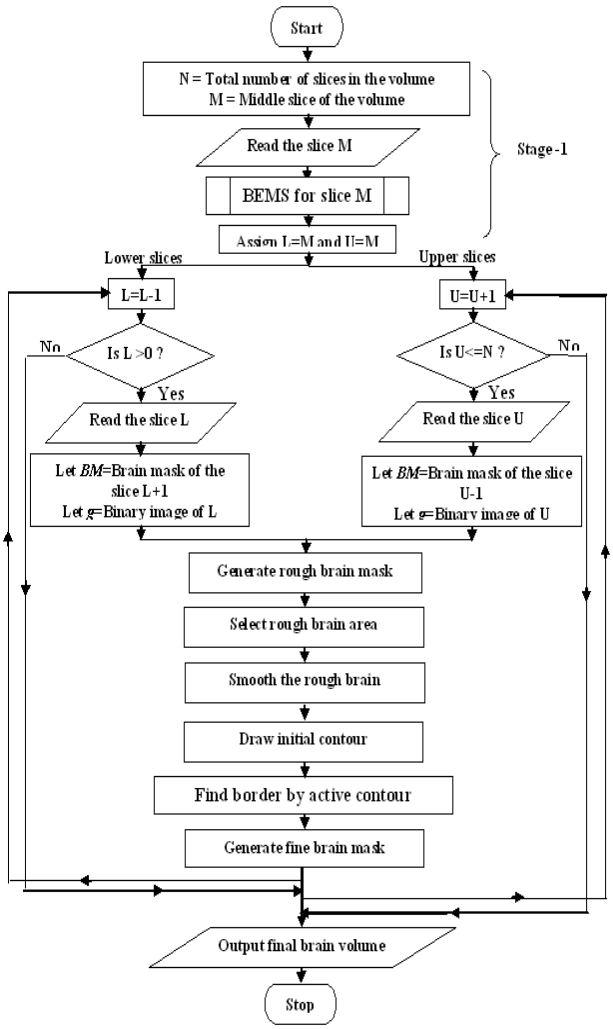

Figure 3: Flowchart of the proposed system

In stage-2 of the proposed method, the input slice is converted to binary form. Then using the previous adjacent brain mask *BM*, the rough brain mask g_{RBM} is generated. After obtaining the rough brain mask we select the rough brain area g_{RB}. Then the rough brain g_{RB} is smoothed to get smoothed rough brain g_{SRB} image.

In our method the process of extracting the brain portions in the remaining slices were simplified based on the similarities of the adjacent slice. Therefore, the radius for the IC for the current slice *g* is calculated using the previous brain mask BM by eqn. (5). We then draw the IC on g_{SRB} to obtain g_{IC}. Then we find the brain border image g_{BB} using the CV method as given in eqns.(6-8). The holes in the brain border image g_{BB} are filled and it is used to extract the CC inside the hole filled brain border image g_{HBB} that overlaps with IC as the brain portion.

Our algorithm propagates from the middle slice and moves to lower slices, and then move from middle slice to upper slices, one direction at a time and produce the brain portion of each slice. After processing all the 2D slices, the skull stripped result of a 3D brain volume is obtained. The detailed algorithm for Stage-2 is:

Step-1: Let *g* be the binary form of the current slice obtained by eqn. (1)
Let *BM* be the brain mask of the previous adjacent slice

Step-2: Label each connected regions in *g* with numbers 1,2,3,…etc., to get g_L. Generate the rough brain mask g_{RBM} by combining all the connected regions that overlap with the previous BM by using the following procedure:

```
let n = max( g_L )
RCOUNT=0
for i=1 to n
        if g(x,y)∩BM(x,y)≠0 then
        {
          RCOUNT=RCOUNT+1;
          R[RCOUNT]= g_L(x, y)
        }
next i
```

g_{RBM} = Union of R[RCOUNT] regions.

Here R(i) represents the different connected regions.

Step-3: Find the rough brain g_{RB} using the following equation.

$$g_{RB} = \begin{cases} f(x,y) & if\ g_{RBM}(x,y) = 1 \\ 0 & otherwise \end{cases} \quad (11)$$

Step-4: Smooth the rough brain g_{RB} using circular average filter to get g_{SRB}.

Step-5: Calculate the radius for IC by eqn. (5) using the previous brain mask *BM* and obtain g_{IC}.

Step-6: Then apply the CV model on g_{SRB} using eqns.(6-8) to obtain brain border image g_{BB} and the holes in the g_{BB} is filled using hole filling algorithm [22] to produce g_{HBB}. The fine brain mask g_{FBM} is generated by finding the intersecting CC regions between g_{HBB} and g_{IC} by eqn. (9).

Step-7: Select the fine brain portion g_{FB} using the fine brain mask g_{FBM} using eqn.(10).

2.1.3. Performance evaluation metrics

To evaluate the performance of the proposed method we make use of Jaccard similarity (*J*), Dice similarity (*D*), Sensitivity (*S*), Specificity (*SP*), False positive rate (*FPR*), and False negative rate (*FNR*). The Jaccard coefficient (J) [24] is given by:

$$J(S_1, S_2) = \frac{|S_1 \cap S_2|}{|S_1 \cup S_2|} = \frac{TP}{TP + FP + FN} \quad (12)$$

The Dice coefficient (D) [25] is given by:

$$D(S_1, S_2) = \frac{2|S_1 \cap S_2|}{|S_1| + |S_2|} = \frac{2TP}{2TP + FP + FN} \quad (13)$$

where, S_1 represents the total pixels of the image obtained by the proposed method and S_2 represents the total pixels in the image obtained from ground truth data. *TP* and *FP* are true positive and false positive, which are defined as the number of voxels correctly and incorrectly classified as brain tissue by the proposed automated method. *TN* and *FN* are true negative and false negative, which are defined as the number of voxels correctly and incorrectly classified as non-brain tissue by the proposed method.

For quantitative evaluation, we also compute the sensitivity (*S*) and specificity (*SP*) and are given by:

$$S = \frac{TP}{TP + FN} \quad (14)$$

$$SP = \frac{TN}{TN + FP} \quad (15)$$

The parameter *S* and *SP* are computed between the 'gold standard" and the corresponding portions extracted by the proposed method. The sensitivity is the percentage of pixels recognized correctly as brain pixels by the proposed method. The specificity is the percentage of pixels recognized correctly as non-brain pixels by the proposed method.

The segmentation errors [3] false positive rate (*FPR*) and false negative rate (*FNR*) are used to measure the misclassification done by the proposed method. *FPR* is the number of pixels incorrectly classified as brain portion and *FNR* is the number of pixels incorrectly classified as non-brain portion by the automated algorithm and are given by:

$$FPR = 1 - SP = \frac{|FP|}{|TN| + |FP|} \quad (16)$$

$$FNR = 1 - S = \frac{|FN|}{|TP| + |FN|} \quad (17)$$

The FPR represents the degree of under segmentation and the FNR the degree of over segmentation.

2.2. Materials

We have used 20 volumes of T1-weighted, 20 volumes of T2-weighted and 20 volumes of PD weighted normal and abnormal MR brain images obtained from the following sources for our experiments.

Twenty volumes of T1-weighted images were obtained from the Internet Brain Segmentation Repository (IBSR) [26] and Twenty volumes of T2 and twenty volumes of PD normal and abnormal subjects used in our experiments were collected from the website 'The Whole Brain Atlas' (WBA) [27].

III. Results and Discussion

We carried out experiments by applying the proposed method on the selected T1, T2 and PD weighted images and performed quantitative and qualitative analysis. Samples of the brain extracted result by the proposed method for T1, T2 and PD weighted images are shown in Figure 4, Images 1 and 2 are T1 weighted images. A T2 weighted images are shown in Image 3 and Image 4 and PD weighted are given in Image 5 and Image 6. In Figure 4, the curvature evolution result obtained using CV method on 50^{th} and 150^{th} iteration was also shown. In this method the maximum number of iteration is assigned as 300. For quantitative analysis, the Jaccard (J) and Dice (D) were calculated for the sample selected images of IBSR dataset using the Eqns.(12) and (13) and are given in Table 1 and Figure 5. In addition, the values J and D computed by using the popular skull stripping methods BET, BSE for the selected images are also given.

To compare the performance of the proposed method Sensitivity (S), Specificity (SP), False positive rate (FPR) and False negative rate (FNR) were also calculated using the eqns.(14)-(17) for the images shown in Figure 5 are given in Table 2. For these selected slices in Figure 5, BET extremely over estimates the brain by including non-brain tissues and BSE included some nonbrain portions and it also failed to extract brain portions in Image 1, Image 8 and Image 9. It can be seen from the Table 2 that the proposed method gives the best average values 0.92, 0.96, 0.98, 0.99 and 0.003 for D, J, S, SP and FPR respectively. The best average value for FNR is 0.003 by BET. Thus from Figure 5 and Table 1 and 2, we observe that the proposed method performs better than BET and BSE.

IV. Conclusion

In this paper, we proposed a skull stripping method based on Chan-Vese active contour model. This is an automatic method for skull stripping in T1, T2 and PD weighted MRI brain images. The proposed method is quantitatively and qualitatively evaluated using IBSR and WBA datasets. The performance of the proposed method is found to be better than that of the existing popular methods BET and BSE.

TABLE I
COMPUTED VALUES FOR THE PARAMETERS JACCARD (J) AND DICE (D) FOR THE IMAGES IN FIGURE 5 FOR BET, BSE AND PROPOSED METHODS.

	Jaccard (J) Similarity			*Dice (D) Similarity*		
Image Name	*BET*	*BSE*	*Proposed*	*BET*	*BSE*	*Proposed*
Image 1	0.4370	0.0084	**0.9267**	0.6082	0.0167	**0.9620**
Image 2	0.8180	0.7224	**0.9033**	0.8999	0.8388	**0.9492**
Image 3	0.8423	0.7751	**0.8797**	0.9144	0.8733	**0.9360**
Image 4	0.8446	0.7577	**0.9352**	0.9158	0.8621	**0.9665**
Image 5	0.8621	0.8635	**0.9694**	0.9259	0.9267	**0.9845**
Image 6	0.8572	0.8457	**0.9337**	0.9231	0.9164	**0.9657**
Image 7	0.6727	0.3613	**0.8635**	0.8043	0.5308	**0.9267**
Image 8	0.4836	0.0017	**0.9503**	0.6519	0.0034	**0.9745**
Image 9	0.3001	0.0005	**0.8712**	0.4617	0.0009	**0.9312**
Image 10	0.8242	0.8556	**0.9213**	0.9037	0.9222	**0.9590**

TABLE 2
COMPUTED AVERAGE VALUES *J, D, S, SP, FPR*, AND *FNR* FOR BET, BSE AND THE PROPOSED METHODS FOR THE IMAGES IN FIGURE 5.

Methods	*J*	*D*	*S*	*SP*	*FPR*	*FNR*
BET	0.69	0.80	0.97	0.94	0.058	**0.003**
BSE	0.52	0.59	0.72	0.96	0.033	0.354
Proposed	**0.92**	**0.96**	**0.98**	**0.99**	**0.003**	0.059

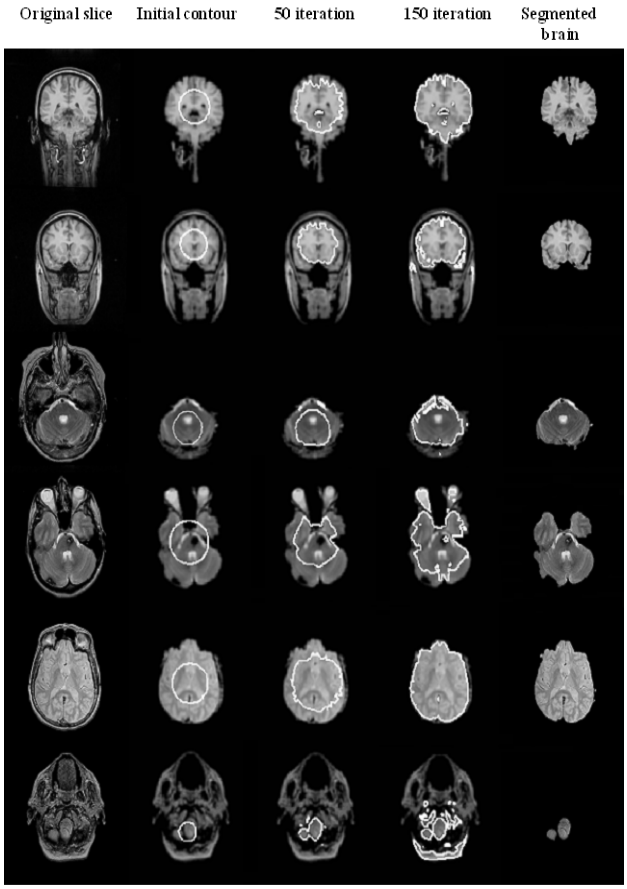

Figure 4: Brain portion extracted by the proposed method. Column 1 original image, column 2 is the initial contour, column 3 & 4 show the evolving contour on 50^{th} and 150^{th} iterations and column 5 is the extracted brain portion.

V. Acknowledgement

This work is partly supported by a research grant by University Grants Commission (UGC), New Delhi (Grant no: M.R.P, F.No-37-154/2009(SR)).

VI. References

[1] E.M. Haacke, R.W. Brown, M.R. Thompson and R. Venkatesan, Magnetic Resonance Imaging: Physical Principles and Sequence Design, John Wiley & Sons, New York (1999).

[2] R.P. Woods, S.T.Grafton, J.D.G. Watson, N.L. Sicotte and J.C. Mazziotta, Automated Image Registration: II Intersubject Validation of Linear and Nonlinear Models. J. of Computer Assisted Tomography, vol. 22, no. 1, pp. 153-165 (1998).

[3] J.M. Lee, U.Yoon, S.M. Nam, J.H. Kim, I.Y. Kim and S.I. Kim, Evaluation of Automated and Semi-automated Skull-stripping Algorithms using Similarity Index and Segmentation Error., Computers in Biology and Medicine, vol. 33, no. 6, pp. 495-507 (2003).

[4] M.S. Atkins, K. Siu, B. Law, J.J. Orchard and W.L. Rosenbaum, Difficulties of T1 Brain MRI Segmentation Techniques, Medical Imaging, Proceedings of SPIE, vol.4684, no.1, pp.1837-1844 (2002).

[5] S.M. Smith, Fast Robust Automated Brain Extraction, Human Brain Mapping, vol.17, no.3, pp. 143-155 (2002).

[6] D.W. Shattuck, S.R. Sandor-Leahy, K.A. Schaper, D.A. Rottenberg and R.M. Leahy, Magnetic Resonance Image Tissue Classification using a Partial Volume Model, Neuroimage, vol.13, no.5, pp. 856-876 (2001).

[7] H. K. Hahn and H.O. Peitgen, The Skull Stripping Problem in MRI Solved by Single 3D Watershed Transform, Proc. of Medical Image Computing and Computer Assisted Intervention (MICCAI), LNCS, vol. 1935, pp. 134-143 (2000).

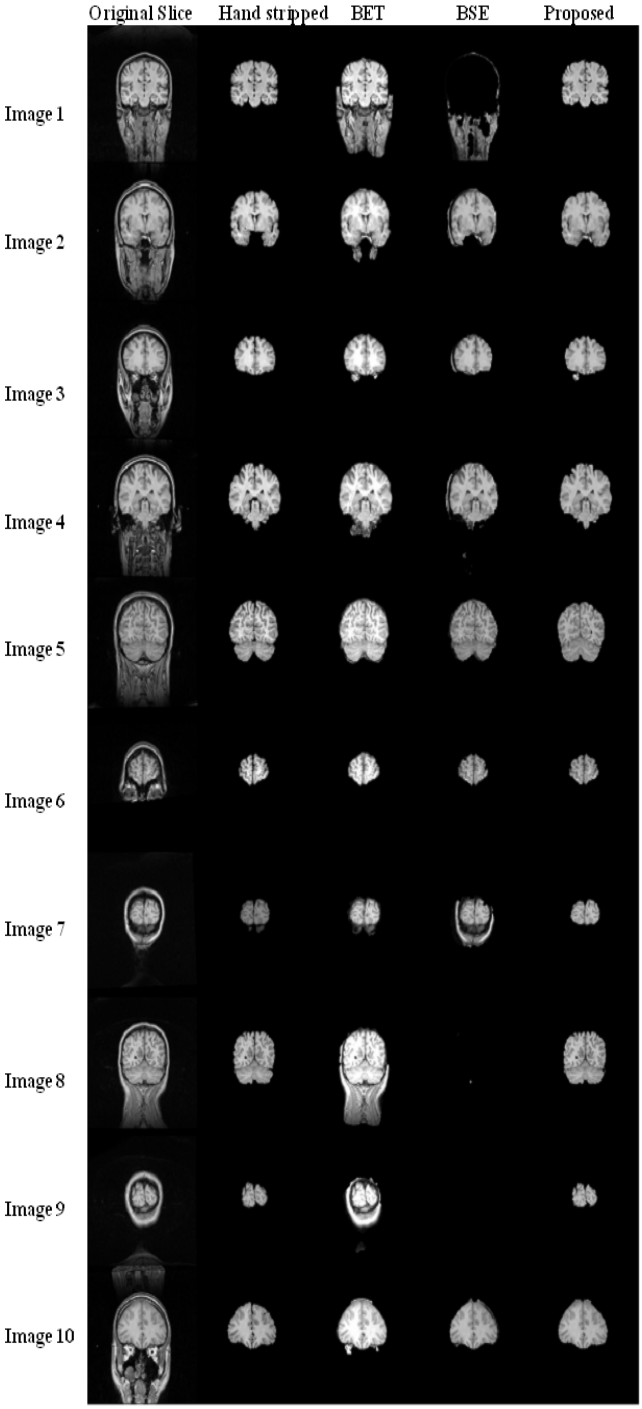

Figure 5 Brain portion extracted using the existing and proposed method for the selected slices from IBSR dataset. Column 1 shows original T1 scans, column 2 hand stripped images, column 3 brain extraction by BET, column 4 by the proposed method, and column 5 by BSE

[8] F. Segonne, A.M. Dale, E. Busa, M. Glessner, D. Salat, H.K. Hahn and B. Fischl, A Hybrid Approach to the Skull Stripping Problem in MRI, Neuroimage, vol. 22, pp. 1060-1075 (2004).

[9] A.H. Zhuang, D.J. Valentino and A.W. Toga, Skull Stripping Magnetic Resonance Images using a Model-based Level Sets, NeuroImge, vol. 32, pp. 79-92, (2006).

[10] A.S. Suresh, W. Zheng, W.L.C. Michael, W.L.Chee and Z. Vitali, Skull Stripping using Graph Cuts, Neuroimage , vol. 49, pp. 225-239 (2009).

[11] Z. Lao, D. Shen and C. Davatzikas, Statistical Shape Model for Automatic Skull-stripping of Brain Images, IEEE International Symposium on Biomedical Imaging, Washington, D.C., pp. 855-858 (2002).

[12] G.J. Park and C. Lee, Skull Stripping Based on Region Growing for Magnetic Resonance Images, Neuroimage, vol. 47, pp. 1394-1407 (2009).

[13] K. Somasundaram and T. Kalaiselvi, Fully Automatic Brain Extraction Algorithm for Axial T2-Weighted Magnetic Resonance Images, Computers in Biology and Medicine, vol. 40, pp. 811-822 (2010).

[14] T. Kalaiselvi, Development of Fully Automatic Brain Extraction Methods for Magnetic Resonance Imaging (MRI) Head Scans and Detection of Abnormality in Brain, Ph.D. Thesis, Gandhigram Rural Institute – Deemed University, Gandhigram, India (2010).

[15] M.E. Brummer, Hough Transforms Detection of the Longitudinal Fissure in Tomographic Head Image, IEEE Transaction on Medical Imaging, vol. 10, no.1, pp. 74-81 (1991).

[16] J. Gao and M. Xie, Skull Stripping MR Brain Images using Anisotropic Diffusion Filtering and Morphological Processing, International Symposium on Computer Network and Multimedia Technology, Wuhan, vol. 1. pp. 1-4 (2009).

[17] W. Zhao, M. Xie, J. Gao and T. Li, A Modified Skull Stripping Method Based on Morphological Processing, Second International Conference on Computer Modeling and Simulation, Sanya, Hainna, vol.1, pp. 159-163 (2010).

[18] K.J. Shanthi and M. Sasikumar, Skull Stripping and Automatic Segmentation of Brain MRI using Seed Growth and Threshold Techniques, International Conference on Intelligent and Advanced Systems, Kuala Lumpur, vol.1, pp. 422-426 (2007).

[19] S. Kobashi, F.Y. Moto, M.D. Ogawa, K. Ando, R. Ishikura, S.H. Kando and Y. Katy, Fuzzy-ASM Based Automated Skull Stripping Method from Infantile Brain MR Images, IEEE International Conference on Granular Computing, San Jose, California, vol.1, pp. 632-635 (2007).

[20] X. Tao and M.C, Chang, A Skull Stripping Method using Deformable Surface and Tissue Classification, Medical Imaging, Proc. SPIE, vol. 7, pp. 623-630 (2010).

[21] N. Otsu, A Threshold Selection Method from Gray-level Histogram, IEEE Transaction on System, Man. and Cybernetics, vol.9. no.1 .pp. 62-66 (1979).

[22] R.C. Gonzalez, and R.E. Woods, Digital Image Processing, Addison-Wesley Publishing Company (1992).

[23] T. Chan and L. Vese, Active Contours without Edges, IEEE Trans. Image Proc., vol. 10. pp. 266-277 (2001).

[24] P. Jaccard, The Distribution of Flora in Alpine Zone, New Phytol, vol. 11, no. 2, pp. 37-50 (1912).

[25] L. Dice, Measures of the Amount of Ecologic Association between Species, Ecology, vol. 26, pp. 297–302 (1945).

[26] IBSR data set available online: http://www.cma.mgh.havard.edu/ibsr/index.html

[27] WBA (Whole Brain Atlas) MR brain image available online: http://www.med.harvad.edu/AANLIB/home.html